A&A 571, A36 (2014)
DOI: 10.1051/0004-6361/201424066

Astronomy & Astrophysics

M dwarfs in the b201 tile of the VVV survey

Colour-based selection, spectral types and light curves⋆

Bárbara Rojas-Ayala[1], Daniela Iglesias[2], Dante Minniti[3,4,5,6], Roberto K. Saito[7], and Francisco Surot[3]

[1] Instituto de Astrofísica e Ciências do Espaço, Universidade do Porto, CAUP, Rua das Estrelas, 4150-762 Porto, Portugal
e-mail: babs@astro.up.pt
[2] Departamento de Física y Astronomía, Facultad de Ciencias, Universidad de Valparaíso, Avenida Gran Bretaña 1111, 2360102 Valparaíso, Chile
[3] Departamento de Astronomía y Astrofísica, Pontificia Universidad Católica de Chile, Vicuña Mackenna 4860, Casilla 306, Santiago 22, Chile
[4] Millennium Institute of Astrophysics, Av. Vicuña Mackenna 4860, 782-0436 Macul, Santiago, Chile
[5] Vatican Observatory, 00120 Vatican City State, Italy
[6] Departamento de Ciencias Físicas, Universidad Andrés Bello, República 220, 837-0134 Santiago, Chile
[7] Universidade Federal de Sergipe, Departamento de Física, Av. Marechal Rondon s/n, 49100-000 São Cristóvão, SE, Brazil

Received 25 April 2014 / Accepted 2 September 2014

ABSTRACT

Context. The intrinsically faint M dwarfs are the most numerous stars in the Galaxy, have main-sequence lifetimes longer than the Hubble time, and host some of the most interesting planetary systems known to date. Their identification and classification throughout the Galaxy is crucial to unraveling the processes involved in the formation of planets, stars, and the Milky Way. The ESO Public Survey VVV is a deep near-IR survey mapping the Galactic bulge and southern plane. The VVV b201 tile, located in the border area of the bulge, was specifically selected for the characterisation of M dwarfs.

Aims. We used VISTA photometry to identify M dwarfs in the VVV b201 tile, to estimate their subtypes, and to search for transit-like light curves from the first 26 epochs of the survey.

Methods. UKIDSS photometry from SDSS spectroscopically identified M dwarfs was used to calculate their expected colours in the $YJHK_s$ VISTA system. A colour-based spectral subtype calibration was computed. Possible giants were identified by a $(J - K_s, H_J)$ reduced proper motion diagram. The light curves of $12.8 < K_s < 15.8$ colour-selected M dwarfs were inspected for signals consistent with transiting objects.

Results. We identified 23 345 objects in VVV b201 with colours consistent with M dwarfs. We provided their spectral types and photometric distances, up to ~300 pc for M9s and ~1.2 kpc for M4s, from photometry. In the range $12 < K_s < 16$, we identified 753 stars as possible giants out of 9232 M dwarf candidates. While only the first 26 epochs of VVV were available, and 1 epoch was excluded, we were already able to identify transit-like signals in the light curves of 95 M dwarfs and of 12 possible giants.

Conclusions. Thanks to its deeper photometry (~4 mag deeper than 2MASS), the VVV survey will be a major contributor to the discovery and study of M dwarfs and possible companions towards the centre of the Milky Way.

Key words. surveys – stars: fundamental parameters – stars: low-mass – Galaxy: bulge

1. Introduction

Stars with masses less than 0.6 $M_\odot$ span the peak of the stellar initial mass function and their numbers dominate the galactic stellar populations (Bastian et al. 2010). These objects are the M dwarfs: cool and faint stars, with complex spectra characterised by molecular absorption of TiO, CaH, and VO in the optical, and FeH and H_2O in the near infrared (Morgan et al. 1943; Mould 1976). Their main sequence lifetimes are longer than the age of the universe, with the least massive ($M_\star < 0.25\ M_\odot$) remaining fully convective during their evolution (Laughlin et al. 1997). Some of them exhibit strong magnetic fields that can produce more magnetic activity that the sun (Johns-Krull & Valenti 1996). They are the hosts of the closest rocky planets to the Earth, and overall, they should be the most likely hosts of terrestrial planets in the Galaxy (Bonfils et al. 2013; Dressing & Charbonneau 2013; Kopparapu 2013; Tuomi et al. 2014).

In the past decade, the study of M dwarfs has greatly benefited from photometric optical and near-infrared wide field deep surveys, such as the Sloan Digital Sky Survey (SDSS, York et al. 2000), the Two Micron All Sky Survey (2MASS, Skrutskie et al. 2006), and the UKIRT Infrared Deep Sky Survey (UKIDSS, Lawrence et al. 2007). Such surveys have found nearby new low-mass and ultra cool dwarfs by colour-selection and proper motion searches (e.g. Kirkpatrick et al. 1997; Deacon et al. 2009; Lodieu et al. 2012c), have provided fundamental properties of a large number of low-mass stars from colour-based relations (e.g. parallaxes and spectral types; Hawley et al. 2002), have enlightened their magnetic activity (e.g. West et al. 2004; Morgan et al. 2012) and flaring properties (e.g. Liebert et al. 1999; Hilton et al. 2010; Davenport et al. 2012), and have allowed the measurements of mass and luminosity functions of low-mass dwarfs in the Galactic disk (Covey et al. 2008; Bochanski et al. 2010), as

⋆ Full Table 3 is only available at the CDS via anonymous ftp to cdsarc.u-strasbg.fr (130.79.128.5) or via http://cdsarc.u-strasbg.fr/viz-bin/qcat?J/A+A/571/A36 well as the photometric initial mass function from Galactic clusters (e.g. Lodieu et al. 2012a,b; Boudreault et al. 2012; Lodieu 2013).

Of the mentioned surveys, only 2MASS has mapped the Milky Way bulge down to magnitude ~14, in two epochs. VISTA Variables in the Vía Láctea (VVV) is a public ESO near-infrared variability survey aimed at scanning the Milky Way bulge and an adjacent section of the mid-plane (Minniti et al. 2010). VVV complements previous near-infrared surveys, providing better spatial resolution and deeper photometry (~4 mag deeper than 2MASS) and multi-epoch K_s-band images which allows the identification of nearby faint/late M dwarfs as well as faraway unknown early M dwarfs with variable photometry consistent with transiting companions (Saito et al. 2011).

We present a colour-based selection of M dwarfs in the b201 tile of the VVV survey. In Sect. 2, we give a description of the survey and of the tile b201. In Sect. 3, we present our M dwarf selection method based on six colour-selection cuts obtained from SDSS spectroscopically observed M dwarfs with UKIDSS photometry. A spectral subtype calibration based on $(Y - J)$, $(Y - K_s)$, and $(H - K_s)$ is given in Sect. 4. In Sect. 5, we identify possible giant contaminants from a reduced proper motion criterion and colour cuts. In Sect. 6, we identify M dwarf candidates with transit-like light curves. We discuss our results and conclusions in Sect. 7.

2. Data

The VVV survey gives near-infrared multicolour information in five passbands, Z (0.87 μm), Y (1.02 μm), J (1.25 μm), H (1.64 μm), and K_s (2.14 μm), and complements surveys such as 2MASS (Skrutskie et al. 2006), DENIS (Epchtein et al. 1997), GLIMPSE II (Churchwell et al. 2005), VPHAS+ (Drew et al. 2013), MACHO (Alcock et al. 1993), OGLE (Udalski et al. 1992), EROS (Aubourg et al. 1993), MOA (Muraki et al. 1999), and GAIA (Perryman et al. 2001). The survey covers a 562 square degree area in the Galactic bulge and the southern disk which contains ~10^9 point sources (Saito et al. 2012a). Each unit of VISTA observations is called a (filled) tile, consisting of six individual (unfilled) pointings (or pawprints) and covers a 1.64 deg^2 field of view. To fill up the VVV area, a total of 348 tiles are used, with 196 tiles covering the bulge (a 14×14 grid) and 152 for the Galactic plane (a 4×38 grid) (Saito et al. 2012b). We selected one specific tile from the bulge to characterise M dwarf stars called "b201". The galactic coordinates of this tile's centre are $l = 350.74816$ and $b = -9.68974$. This tile is located in the border region of the bulge where the star density is lower. The total extinction in this tile is expected to be mostly in the background of the M dwarfs, and therefore overestimated. However, the mean extinction over the entire tile is $A_{K_s} = 0.0083$ mag (Fig. 1) and, therefore, the effect of extinction should be negligible allowing good photometry (the effect would be significant in other more reddened regions of the bulge as shown by the reddening maps of Gonzalez et al. 2012).

Photometric catalogues for the VVV images are provided by the Cambridge Astronomical Survey Unit (CASU[1]). The catalogues contain the positions, fluxes, and some shape measurements obtained from different apertures, with a flag indicating the most probable morphological classification. In particular, we note that "–1" is used to denote the best-quality photometry of stellar objects (Saito et al. 2012b). Some other flags are "–2" (borderline stellar), "0" (noise), "–7" (sources containing bad pixels), and "–9" (saturated sources).

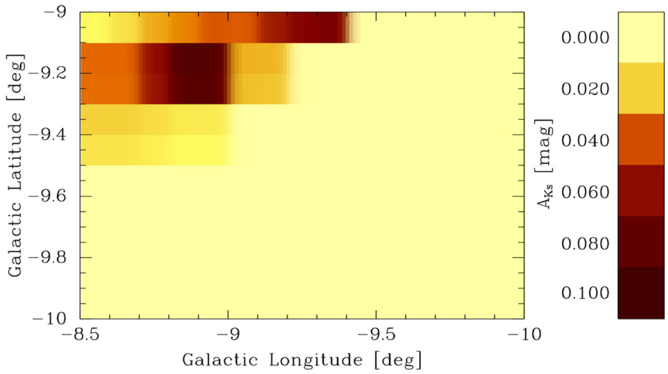

Fig. 1. Extinction map of the VVV field b201. The values are based on the maps of Gonzalez et al. (2012), using the Cardelli et al. (1989) extinction law, for a resolution of $6' \times 6'$. This field is located in the bottom-right corner of the VVV bulge area, within coordinates $-10° \lesssim l \lesssim -8.5°$ and $-10° \lesssim l \lesssim -9°$. For a large portion of the area the total extinction A_{K_s} is lesser than the lower limit computed by the Gonzalez et al. (2012) map, of $A_{K_s} < 0.0001$ mag. While the maximum value found is $A_{K_s} = 0.0890$ mag, the mean extinction over the entire field is $A_{K_s} = 0.0083$ mag. This degree of extinction produces no or negligible effects in the photometric limits used in our target selection.

3. Colour-selection cuts from SDSS-UKIDSS M dwarfs

To identify potential M dwarfs in the VVV b201 tile, we performed several colour-selection cuts using the VVV passbands as described in the subsections below. Before performing those cuts, we did a pre-selection of the objects in the tile b201 to ensure that the objects have the best-quality photometry. In this pre-selection, we included only objects that had photometry in all five passbands ($ZYJHK_s$), and that were classified as stellar (flag "–1") in each passband. A total of 142 321 objects in the tile b201 satisfied these conditions.

The colour selection cuts were defined from spectroscopically identified M dwarfs with UKIRT Infrared Deep Sky Survey (UKIDSS) photometry.

We selected the Sloan Digital Sky Survey DR7 Spectroscopic M dwarf catalogue by West et al. (2011) as the comparative M dwarf sample. The 70 841 M dwarf stars in this catalogue had their optical spectra visually inspected and the spectral type of each object was assigned by comparing them to spectral templates. Their spectral types range from M0 to M9, with no half subtypes. This catalogue also provides values for the CaH2, CaH3 and TiO5 indices, which measure the strength of CaH and TiO molecular features present in the optical spectra of M dwarfs.

We performed a cone search with a radius of 5″ of these SDSS M dwarf stars in the UKIDSS-DR8 survey (Lawrence et al. 2012). The UKIDSS survey is carried out using the Wide Field Camera (WFCAM), with a Y (1.0 um), J (1.2 um), H (1.6 um) and K (2.2 um) filter set. The cone search provided UKIDSS-DR8 matches for almost half of the SDSS M dwarf sample (34 416 matches). Next, we only kept the UKIDSS counterparts consistent with being a stellar objects (pStar > 0.9), with measured magnitudes in all WFCAM $YJHK$ filters, and with CaH and TiO indices compatible with average M dwarf stars. The final SDSS-UKIDSS comparative M dwarf sample consists of 17 774 objects.

To convert the WFCAM $YJHK$ magnitudes of the SDSS-UKIDSS M dwarf sample to VISTA $YJHK_s$ magnitudes, we

[1] http://apm49.ast.cam.ac.uk/

Table 1. VISTA mean colours and standard deviations per spectral subtype.

Sp.T.	$\overline{Y-J}$	$\overline{Y-H}$	$\overline{Y-K_s}$	$\overline{J-H}$	$\overline{J-K_s}$	$\overline{H-K_s}$	No. of stars
M0	0.428 ± 0.092	1.039 ± 0.087	1.163 ± 0.063	0.611 ± 0.116	0.734 ± 0.092	0.124 ± 0.079	1946
M1	0.449 ± 0.077	1.047 ± 0.061	1.200 ± 0.064	0.598 ± 0.086	0.751 ± 0.081	0.153 ± 0.046	2520
M2	0.467 ± 0.061	1.042 ± 0.073	1.219 ± 0.058	0.575 ± 0.088	0.752 ± 0.071	0.177 ± 0.058	3043
M3	0.487 ± 0.081	1.043 ± 0.062	1.241 ± 0.064	0.556 ± 0.089	0.754 ± 0.083	0.198 ± 0.038	3293
M4	0.515 ± 0.083	1.057 ± 0.090	1.278 ± 0.068	0.542 ± 0.110	0.762 ± 0.085	0.220 ± 0.075	2872
M5	0.555 ± 0.096	1.092 ± 0.069	1.340 ± 0.082	0.538 ± 0.103	0.786 ± 0.099	0.248 ± 0.044	1264
M6	0.619 ± 0.082	1.150 ± 0.067	1.442 ± 0.076	0.531 ± 0.087	0.823 ± 0.084	0.292 ± 0.033	1224
M7	0.664 ± 0.117	1.198 ± 0.126	1.513 ± 0.136	0.533 ± 0.064	0.849 ± 0.068	0.315 ± 0.037	1141
M8	0.758 ± 0.070	1.304 ± 0.102	1.662 ± 0.122	0.546 ± 0.052	0.904 ± 0.067	0.358 ± 0.033	320
M9	0.850 ± 0.079	1.429 ± 0.114	1.830 ± 0.139	0.579 ± 0.054	0.980 ± 0.071	0.401 ± 0.038	151

used the conversions provided by CASU[2], derived from regions observed with both VISTA and WFCAM.

The mean and standard deviation for all of the colours from VISTA $YJHK_s$ photometry per M spectral subtype, as well as the number of stars considered for their computation, are shown in Table 1.

We have defined the colour-based selection of M dwarf by inspecting the colours of all the stars within 1-sigma from the mean colour. The resulting limits are:

$0.336 < (Y-J)_{\rm VISTA} < 0.929;$
$0.952 < (Y-H)_{\rm VISTA} < 1.544;$
$1.100 < (Y-K_s)_{\rm VISTA} < 1.969;$
$0.432 < (J-H)_{\rm VISTA} < 0.727;$
$0.642 < (J-K_s)_{\rm VISTA} < 1.051;$
$0.045 < (H-K_s)_{\rm VISTA} < 0.438.$

From our pre-selection of 142 321 objects, only 23 345 objects have colours that are consistent with M dwarf stars, according to the colour-cuts shown above. Forty-percent of these objects have magnitudes $12 < K_s < 16$, and therefore have reliable magnitudes for variability and are the best M dwarf candidates to detect any possible transits (9232 objects).

4. Spectral types and photometric distances for VVV M dwarfs

The mean colours per spectral type in Table 1 show that spectral type is a monotonically increasing function for the following colours: $Y-J$, $Y-K_s$, and $H-K_s$. We conducted multivariate regressions on the $Y-J$, $Y-K_s$, and $H-K_s$ colours for the 17 774 stars in the SDSS-UKIDSS comparative M dwarf sample to identify the best-fit relationship to predict each star's spectral type. The resulting subtype calibration is

$$\begin{aligned} \text{Msubtype} &= 5.394(Y–J) + 4.370(Y–J)^2 \\ &\quad + 24.325(Y–K_s) - 7.614(Y–K_s)^2 \\ &\quad + 7.063(H–K_s) - 20.779, \qquad (1) \\ \text{RMSE}_\text{V} &= 1.109, \end{aligned}$$

with $RMSE_V$ being the root-mean-square error of validation, a sensible estimate of average prediction error (see appendix in Rojas-Ayala et al. 2012). Spectral types for all the M dwarf candidates are given in Table 3.

To identify the location of M dwarfs at different distances in the Colour-Magnitude Diagram (CMD), we used the nearby M dwarfs with M_{K_s} and spectral type estimates in Rojas-Ayala et al. (2012). Using the colour transformations from WFCAM

[2] http://apm49.ast.cam.ac.uk/surveys-projects/vista/technical/photometric-properties

Table 2. Average M_{K_s} and K_s at different distances per M subtype.

Sp.T.	M_{K_s}	$(J-K_s)$	$K_s^{60\ \rm pc}$	$K_s^{300\ \rm pc}$	$K_s^{1000\ \rm pc}$
M0	5.240	0.753	9.131	12.626	15.240
M1	5.656	0.773	9.547	13.042	15.656
M2	6.126	0.748	10.017	13.512	16.126
M3	6.681	0.775	10.572	14.067	16.681
M4	7.790	0.788	11.680	15.175	17.790
M5	7.976	0.788	11.866	15.361	17.976
M6	8.980	0.842	12.871	16.366	18.980
M7	9.609	0.901	13.499	16.994	19.609
M8	10.113	0.980	14.003	17.498	20.113
M9	10.589	1.153	14.480	17.975	20.589

to the VISTA system, we estimated the apparent K_s magnitudes at different distances per spectral type (Table 2). The locations of the M dwarf sequence at 60 pc, 300 pc and 1000 pc coincide with the location of the colour-based selection of M dwarfs described in Sect. 3, as well as the K+M dwarf sequence identified by Saito et al. (2012b), as shown in the CMD of Fig. 2. Based on the estimated M subtypes derived by Eq. (1), we provide estimated distances for the colour-based selected M dwarfs in Table 3. We emphasise that these distances are provided to have an approximate location of the objects with respect to the bulge, and they are not expected to be accurate.

Considering the spectral types in Table 3, the deeper photometry of VVV has a higher impact on the number of late type M dwarfs that can be found in the b201 tile. By performing a 5″ search of the 23 345 objects in 2MASS Point Source catalogue (Cutri et al. 2003), we can estimate that the number of M9 stars found by VVV in the b201 tile is ~30 times larger than the one that can be found with only 2MASS photometry (1 versus 30 M9 stars at distances up to ~300 pc). The number of M8 and M7 stars is 18 and 13 times larger that the ones by only 2MASS photometry (at distances up to ~500 pc), while the number of M4 is about 4 times more (at distances up to ~1000 pc).

5. Possible giant contaminants

Giant stars are the most common contaminants of colour-based selections of M dwarfs. Bessell & Brett (1988) derived intrinsic colours in the Johnson-Glass system for several V and III class stars, and schematically showed the position of dwarfs, giants, supergiants, carbon stars and long-period variables in the $(H-K, J-H)$ diagram. By using $(V-K)$ as proxy for spectral type, Bessell & Brett (1988) showed that giants and dwarf stars share similar $(J-H)$ and $(H-K)$ colours for $(V-K) < 3.5$, but their $(H-K)$ colours make them almost indistinguishable up to $(V-K) \sim 6$. Colour cuts based on $(J-K_s)$ and $(J-H)$ colours

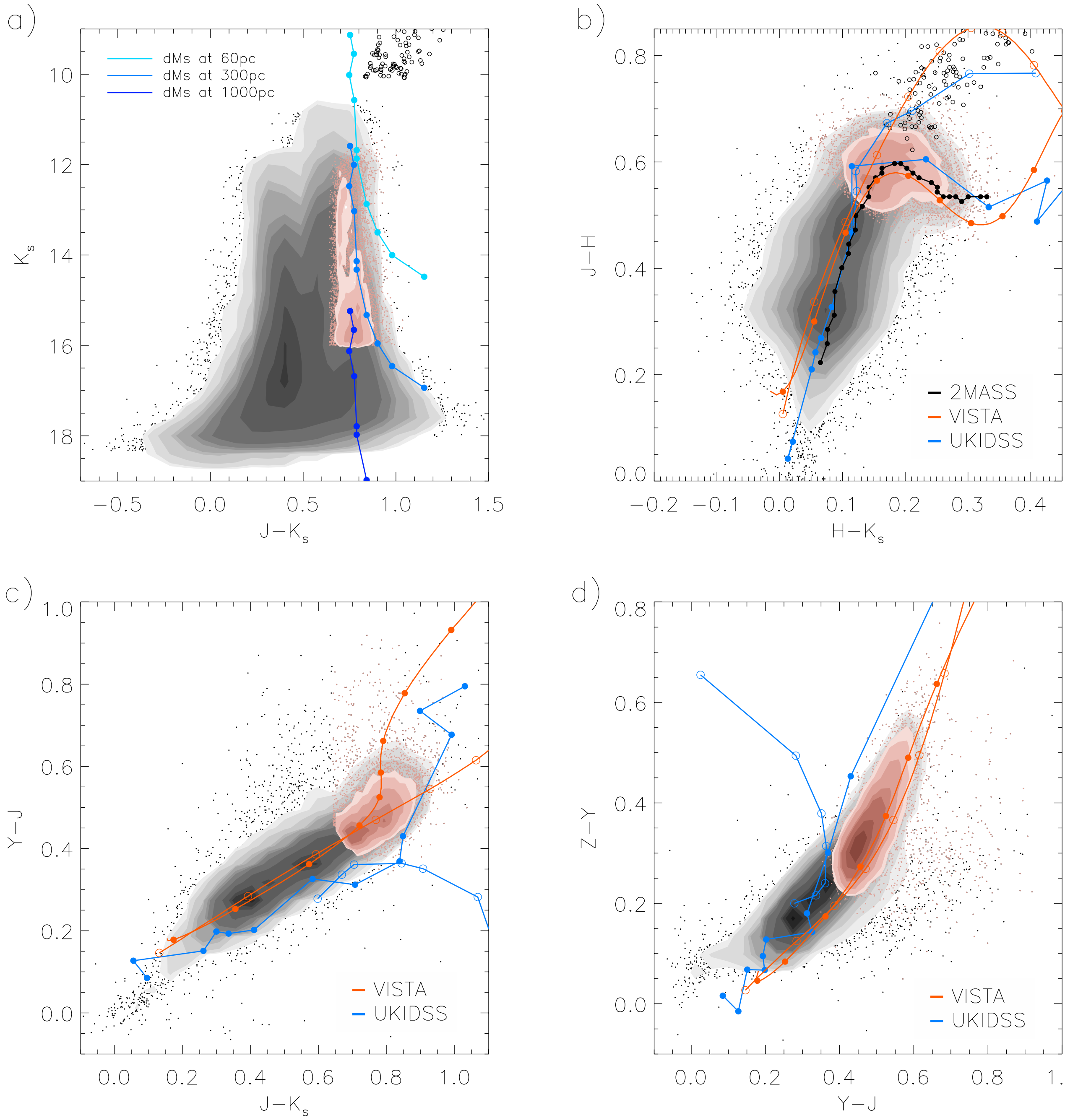

Fig. 2. Colour–magnitude diagram and colour-colour diagrams for objects classified as stellar in the tile b201. The colour-based selection of M dwarfs is shown in pink in all diagrams. Black open circles are giant stars located at similar (l, b) as b201 by the BRaVA Project (Rich et al. 2007; Kunder et al. 2012). **a)** The colour identified M dwarfs fill the region that agrees with the K+M dwarf sequence in the $(J - K_s, K_s)$ CMD of the outermost region in the VVV bulge area, identified by Saito et al. (2012b). The estimated M dwarf spectral sequences at 60 pc, 300 pc, and 1000 pc are shown. **b)–d)** $(H - K_s, J - H)$, $(J - K_s, Y - J)$, and $(Y - J, Z - Y)$ diagrams for all stellar objects with $12 < K_s < 16$ only. The blue lines represent the dwarf (filled circles) and giant (open circles) sequences, based on UKIDSS synthetic colours by Hewett et al. (2006). The orange lines represent the dwarf (filled circles) and giant (open circles) sequences, based on VISTA synthetic colours derived from stars in the IRTF Spectral Library (see Appendix A). In the $(H - K_s, J - H)$ diagram, the black line corresponds to the JHK_s stellar locus by Covey et al. (2007), derived from SDSS and 2MASS photometry), and it is in agreement with the one derived in this work from VISTA synthetic colours. The disagreement between the UKIDSS and VISTA sequences may be due to the differences between the Z and Y synthetic filters of each survey.

have been used to identify giants in different parts of the Galaxy (e.g. Sharma et al. 2010; Bochanski et al. 2014), however they only serve to isolate the cooler giants from M dwarfs ($(J - K_s) > 0.85$). The giant sequence passes through the M dwarf region in the $(J - K_s, J - H)$ diagram, with K and early M giants contaminating the sample of colour identified M dwarfs (see Fig. 2). The colour selection criteria described in Sharma et al. (2010) identifies 299 objects as giants stars in our whole M dwarf sample, 60 of them within the magnitude range $12 < K_s < 16$.

Another way to identify giants, when their distances are unknown, is by their location in a reduced proper motion diagram (e.g. Lépine & Gaidos 2011). To get estimates of the proper motions of the whole M dwarf colour-based selection, we performed a cone search with a 5″ radius of their coordinates in

Table 3. M dwarfs in the VVV b201 tile.

Name	Z mag	Y mag	J mag	H mag	K_s mag	Sp.T.	d pc	$\mathrm{PM_{SPM4}}$ mas/yr	H_J^{SPM4} mag	$\mathrm{PM_{PPMXL}}$ mas/yr	H_J^{PPMXL} mag	Flag
VVVJ17594599-4205194	18.242	17.676	17.105	16.516	16.396	3	877					
VVVJ17594603-4206345	19.523	19.004	18.094	17.467	17.413	8	288					
VVVJ17594628-4206516	18.166	17.964	17.432	16.786	16.638	3	980					
VVVJ17594859-4206457	17.463	17.103	16.599	15.976	15.812	3	670					
VVVJ17594908-4205074	16.729	16.466	16.024	15.399	15.27	2	674			11.987	6.417	
VVVJ17594944-4207152	14.435	14.135	13.744	13.12	12.949	1	287					
VVVJ17594955-4205529	13.493	13.21	12.781	12.173	12.038	1	189	9.173	2.593	9.571	2.686	
VVVJ17594971-4205192	15.525	15.065	14.525	14.0	13.746	4	155			5.345	3.165	
VVVJ17594996-4205371	16.832	16.539	16.098	15.478	15.396	1	887	24.537	8.047			
VVVJ17595034-4207015	18.16	17.711	17.082	16.637	16.381	5	480					
VVVJ17595079-4207372	16.179	15.856	15.375	14.654	14.513	3	368			11.873	5.748	G23
VVVJ17595111-4206312	18.64	18.466	17.919	17.397	17.153	4	746					
VVVJ17595235-4207075	18.284	17.923	17.315	16.798	16.557	5	520					
VVVJ17595271-4207183	18.685	18.308	17.8	17.167	16.871	4	655					
VVVJ17595313-4204316	17.844	17.54	17.076	16.466	16.345	2	1106			5.946	5.947	

Notes. Only a portion of this table is shown here to demonstrate its form and content. The full table is available at the CDS. In column Flag, likely giants are flagged as "G" followed by numbers 1, 2 and/or 3, where 1-proper motion from SPM4, 2-proper motion from PPMXL, and 3-colour selected. Stars with transit-like curves are flagged as "T"

the PPMXL catalogue (Roeser et al. 2010) and the SPM4 catalogue (Girard et al. 2011). The PPMXL catalogue covers both hemispheres, while the SPM4 catalogue covers objects between the south celestial pole and $-20°$ declination, with higher proper motion precision than PPMXL. Both of these catalogues provide the crossmatched 2MASS photometry for their objects, and we only considered the objects with $|K_s^{\mathrm{VISTA}} - K_s^{\mathrm{2MASS}}| \leq 0.5$ mag. We obtained total proper motions, μ in $''$/yr, for 6464 and 2940 objects from PPMXL and SPM4, respectively. The number of stars in the $12 < K_s < 16$ M dwarf selection with PPMXL and SPM4 total proper motions is 6216 and 2760, respectively. We calculated their J magnitude reduced proper motion H_J using the definition

$$H_J = J + 5\log_{10}\mu. \quad (2)$$

Lépine & Gaidos (2011) defined a criterion to separate M dwarfs from giants based on V magnitude, reduced proper motion H_V, and $(V - J)$ colour. This criterion cannot be used for our stars since V magnitudes are hard to find in the literature for the $12 < K_s < 16$ M dwarfs. For that reason, we computed an equivalent criterion based on J and K_s magnitudes. We grouped the stars of the Lépine & Gaidos (2011) study by their estimated spectral types, obtained their mean $(V - J)$ and $(J - K_s)$ colours, and calculated the dwarf/giant discriminator H_J^* as a function of mean $(V - J)$ per spectral type, using our definition of H_J, by rewriting Eq. (8) of Lépine & Gaidos (2011) as follows:

$$H_J^* = 1.5(V - J) - 3.0. \quad (3)$$

Then, using the mean $(J-K_s)$ colour corresponding to each mean $(V - J)$ per spectral type, we performed a linear fit to obtain H_J^* as a function of $(J - K_s)$ and, therefore, an equivalent criterion to Eq. (3) based on $(J - K_s)$, instead of $(V - J)$ is:

$$H_J^{\mathrm{dwarf}} > H_J^* = 68.5(J - K_s) - 50.7. \quad (4)$$

In the $12 < K_s < 16$ M dwarf sample, using the criterion above, we identified 555 likely giant stars from PPMXL proper motions, with 24 of them exhibiting $(J - K_s)$ and $(J - H)$ colours compatible with giants. From SPM4 proper motions, we identified 328 likely giants, with 18 of them exhibiting cool giant colours. Almost all of the $12 < K_s < 16$ objects in SPM4 have also PPMXL proper motions (2595 stars). For about 40% of them, the PPMXL and SPM4 total proper motions agree within $\pm 0.01''$/yr, with the PPMXL catalogue providing higher values of total proper motions than SPM4 (by more than $0.01''$/yr) for the majority of the rest. Considering the reduced proper motion criterion, only 164 objects are likely giants with both PPMXL and SPM4 proper motions (16 of them have giants colours, too). Their locations in the CMD and $(H - K_s, J - H)$ diagram are shown in Fig. 3.

The names, VISTA photometry, spectral type, and estimated distances of the 23 345 colour-selected M dwarf candidates are listed in Table 3. The total proper motion, H_J and likely giant flag are given for the stars with PPMXL and SPM4 proper motions, as well as the 299 colour selected giants.

6. VVV light curves for M dwarfs

We constructed the light curves of the 9232 M dwarf candidates with $12 < K_s < 16$ in the tile b201, considering only the first 26 epochs of VVV observations. These epochs cover observations taken from December 2010 to September 2012. Considering the unevenly sampled data and the low number of epochs, we searched for objects with light curves with transit-like signals by identifying outliers, i.e. epochs with magnitudes considerable fainter than the median magnitude of all epochs, in each light curve. We used the median and median absolute deviation (MAD) statistics to identify outliers, given that they are very insensitive to the presence of outliers in the data, contrary to the mean and the standard deviation. An epoch is classified as an outlier if its magnitude is 3-MAD away from the median magnitude of the light curve.

By inspecting the outliers in each light curve, we found that certain epochs were consistently flagged as outliers. These epochs correspond to the observation dates with seeings smaller than $0.8''$, where several stars with $K_s < 12.8$–13 mag appear to be consistently fainter. We also found that epoch 14 exhibits the higher dispersion in all magnitudes. Considering the above, and the fact that at all epochs the dispersion increases at $K_s > 15.8$ mag, we restricted our study of the light curves to the M dwarf candidates with $12.8 < K_s < 15.8$ mag, without considering epoch 14. Given the small number of epochs, we also only considered objects with a "-1" flag (stellar) in all epochs

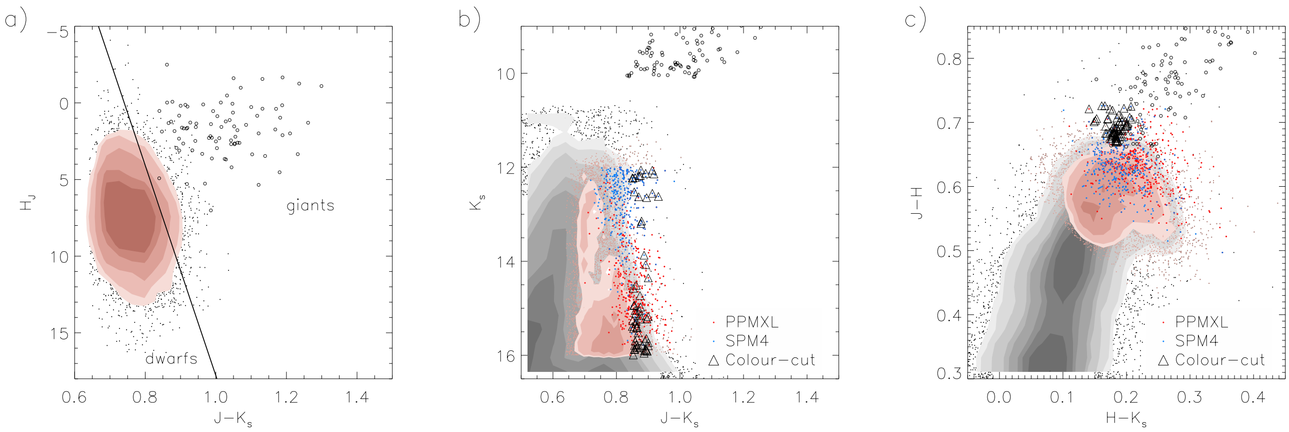

Fig. 3. Reduced proper motion (RPM), colour–magnitude, and $(H - K_s, J - H)$ diagrams for the $12 < K_s < 16$ M dwarfs selected by colour-based relations (pink contours). Bulge giant stars from the BRaVA project are shown as black open circles. **a)** In the RPM diagram, likely giants contaminants lie above the black line which represents the H_J^* as a function of $(J - K_s)$ colour. **b)** In the CMD, likely giant stars from SPM4 (blue dots) exhibit brighter magnitudes attributable to the magnitude cut of the survey, while PPMXL provides parallaxes for fainter likely giants (red dots). Crosses depict likely giants identified by colour-cuts from Sharma et al. (2010). **c)** Likely giants selected by colour-cuts (crosses) follow the trend of the BRaVa giants (open circles) in the $(H - K_s, J - H)$ diagram. Likely giants identified by proper motions are mostly located in the upper part of the M dwarf region (redder $J - H$ colours), and exhibit $H - K_s$ colours redder than ~0.13 mag.

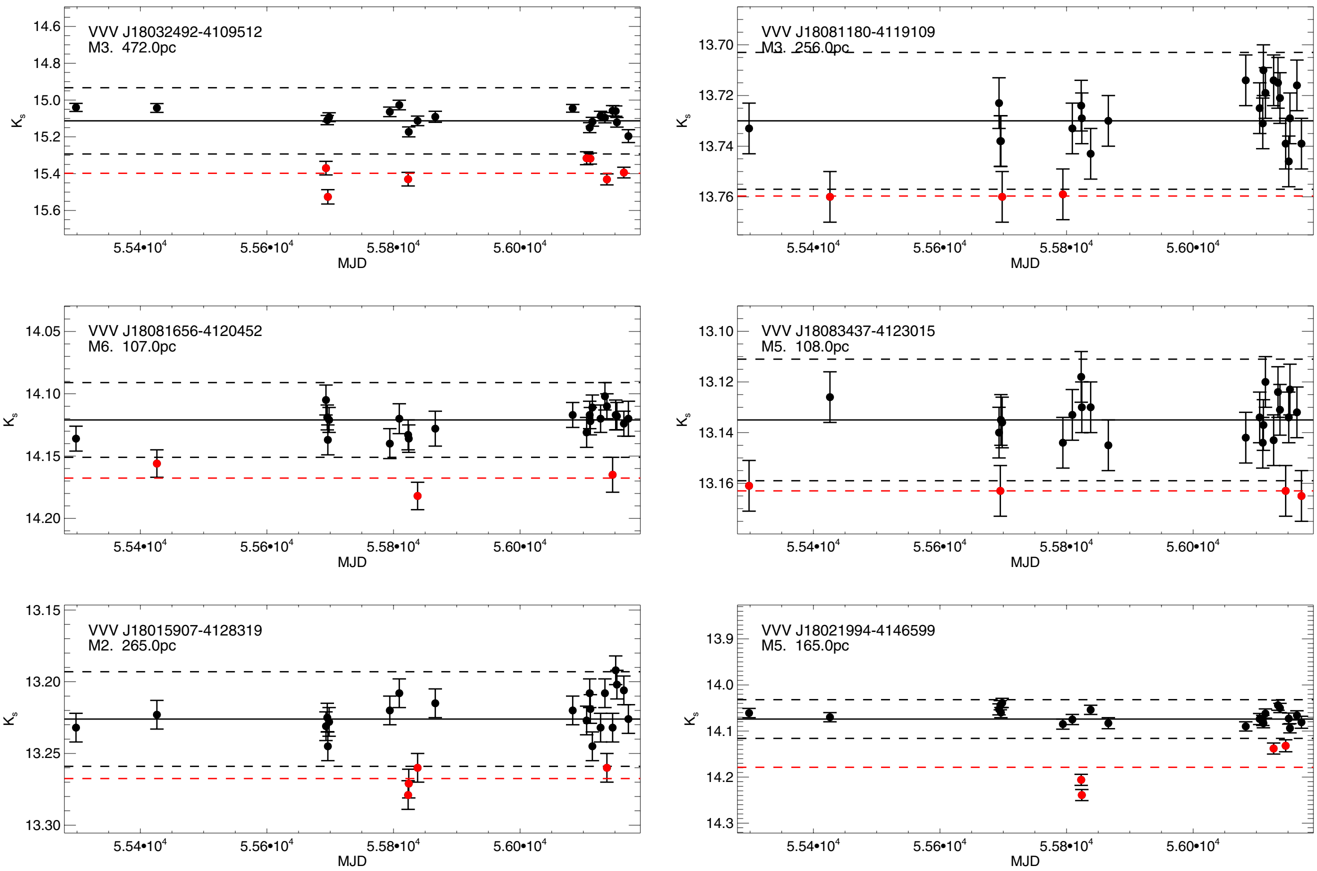

Fig. 4. Light curves of 6 M dwarf candidates. The dotted black lines indicate the ±3-MAD cuts to find the outliers. The red dotted line indicates the mean magnitude of the outliers. Considering the mean magnitude of the outliers and assuming a non-grazing transit, the possible companions have sizes consistent with ultra-cool dwarfs down to terrestrial bodies.

and with mean magnitude errors of all the epochs smaller than or equal to 1.5 MAD.

We found 95 M dwarf candidates and 12 likely giants that exhibit at least 3 epochs with 3-MAD fainter K_s magnitudes than the median of the 25 epochs (removing epoch 14) out of the 3843 objects that satisfied all of the conditions mentioned above. Examples of the type of light curves found can be seen in Fig. 4.

7. Conclusions

We identified 23 345 M dwarf candidates in the VVV b201 tile from colour-cuts based on 17 774 M dwarfs with SDSS spectra and UKIDSS photometry. Their positions in VISTA-colour diagrams match the stellar locus derived from stars with 2MASS photometry by Covey et al. (2007), as well as the dwarf sequences from synthetic colours calculated from IRTF Library spectra (Appendix A). From that sample, we selected 9232 stars with $12 < K_s < 16$ mag for further characterisation of their light curves. From their position on a reduced proper motion diagram and their $J - K_s$ and $J - H$ colours, we identified 753 objects with a higher chance of being giants instead of M dwarfs. From the sample of likely M dwarfs, we searched for transit-like light curves based on 25 epochs of the VVV survey. We found 95 objects with light curves with 3 or more epochs with significant decrease in their luminosity. Assuming that the light curves correspond to non-grazing objects fully transiting the M dwarf, the sizes of these possible companions range from the ones of ultra-cool dwarfs (~0.12) to sizes of a couple of earth radii. However, this is assuming the conditions mentioned above and assuming that the light curves are due to transiting objects. More VVV epochs and further spectroscopic follow-up are needed to confirm the properties of the stars and the real nature of their light curves. The deeper photometry of VVV has a higher impact on the number of nearby, late type M dwarfs that can be found towards the bulge of the Galaxy, missed by previous NIR surveys. VVV will be a major contributor to the discovery and study of very low-mass stars and and possible companions towards the centre of the Milky Way.

Acknowledgements. We would like to thank Karla Peña Ramírez and Ann M. Martin for their help during the preparation of this manuscript. We thank the anonymous referee for her/his helpful comments that improved our manuscript. We gratefully acknowledge use of data from the ESO Public Survey programme ID 179.B-2002 taken with the VISTA telescope, and data products from the Cambridge Astronomical Survey Unit, and funding from the BASAL Center for Astrophysics and Associated Technologies (CATA) PFB-06, from Project IC120009 "Millennium Institute of Astrophysics (MAS)" of Iniciativa Científica Milenio from the Ministerio de Economía, Fomento y Turismo de Chile, and from Proyecto FONDECYT Regular 1130196. B.R-A. acknowledges support from the Fundacão para a Ciêcia e a Tecnologia (FCT, Portugal) through the grant contract SFRH/BPD/87776/2012. R.K.S. acknowledges support from CNPq/Brazil through projects 310636/2013-2 and 481468/2013-7. This work is based in part on data obtained as part of the UKIRT Infrared Deep Sky Survey. This publication makes use of data products from the Two Micron All Sky Survey, which is a joint project of the University of Massachusetts and the Infrared Processing and Analysis Center/California Institute of Technology, funded by the National Aeronautics and Space Administration and the National Science Foundation. This research has made use of the VizieR catalogue access tool, CDS, Strasbourg, France This work used the Tool for OPerations on Catalogues And Tables (TOPCAT) processing software (Taylor 2005).

References

Alcock, C., Allsman, R. A., Axelrod, T. S., et al. 1993, in Sky Surveys, Protostars to Protogalaxies, ed. B. T. Soifer, ASP Conf. Ser., 43, 291
Aubourg, E., Bareyre, P., Brehin, S., et al. 1993, The Messenger, 72, 20
Bastian, N., Covey, K. R., & Meyer, M. R. 2010, ARA&A, 48, 339
Bessell, M. S., & Brett, J. M. 1988, PASP, 100, 1134
Bochanski, J. J., Hawley, S. L., Covey, K. R., et al. 2010, AJ, 139, 2679
Bochanski, J. J., Willman, B., West, A. A., Strader, J., & Chomiuk, L. 2014, AJ, 147, 76
Bohlin, R. C. 2014 [arXiv:1403.6861]
Bonfils, X., Delfosse, X., Udry, S., et al. 2013, A&A, 549, A109
Boudreault, S., Lodieu, N., Deacon, N. R., & Hambly, N. C. 2012, MNRAS, 426, 3419
Cardelli, J. A., Clayton, G. C., & Mathis, J. S. 1989, ApJ, 345, 245
Churchwell, E., Brian, B., Bania, T., et al. 2005, Spitzer Proposal, 20201
Covey, K. R., Ivezić, Ž., Schlegel, D., et al. 2007, AJ, 134, 2398
Covey, K. R., Hawley, S. L., Bochanski, J. J., et al. 2008, AJ, 136, 1778
Cushing, M. C., Rayner, J. T., & Vacca, W. D. 2005, ApJ, 623, 1115
Cutri, R. M., Skrutskie, M. F., van Dyk, S., et al. 2003, VizieR Online Data Catalog: II/246
Davenport, J. R. A., Becker, A. C., Kowalski, A. F., et al. 2012, ApJ, 748, 58
Deacon, N. R., Hambly, N. C., King, R. R., & McCaughrean, M. J. 2009, MNRAS, 394, 857
Dressing, C. D., & Charbonneau, D. 2013, ApJ, 767, 95
Drew, J. E., Barentsen, G., Fabregat, J., et al. 2013, The Messenger, 154, 41
Epchtein, N., de Batz, B., Capoani, L., et al. 1997, The Messenger, 87, 27
Girard, T. M., van Altena, W. F., Zacharias, N., et al. 2011, AJ, 142, 15
Gonzalez, O. A., Rejkuba, M., Zoccali, M., et al. 2012, A&A, 543, A13
Hawley, S. L., Covey, K. R., Knapp, G. R., et al. 2002, AJ, 123, 3409
Hewett, P. C., Warren, S. J., Leggett, S. K., & Hodgkin, S. T. 2006, MNRAS, 367, 454
Hilton, E. J., West, A. A., Hawley, S. L., & Kowalski, A. F. 2010, AJ, 140, 1402
Johns-Krull, C. M., & Valenti, J. A. 1996, ApJ, 459, L95
Kirkpatrick, J. D., Beichman, C. A., & Skrutskie, M. F. 1997, ApJ, 476, 311
Kopparapu, R. K. 2013, ApJ, 767, L8
Kunder, A., Koch, A., Rich, R. M., et al. 2012, AJ, 143, 57
Laughlin, G., Bodenheimer, P., & Adams, F. C. 1997, ApJ, 482, 420
Lawrence, A., Warren, S. J., Almaini, O., et al. 2007, MNRAS, 379, 1599
Lawrence, A., Warren, S. J., Almaini, O., et al. 2012, VizieR Online Data Catalog: II/314
Lépine, S., & Gaidos, E. 2011, AJ, 142, 138
Liebert, J., Kirkpatrick, J. D., Reid, I. N., & Fisher, M. D. 1999, ApJ, 519, 345
Lodieu, N. 2013, MNRAS, 431, 3222
Lodieu, N., Deacon, N. R., & Hambly, N. C. 2012a, MNRAS, 422, 1495
Lodieu, N., Deacon, N. R., Hambly, N. C., & Boudreault, S. 2012b, MNRAS, 426, 3403
Lodieu, N., Espinoza Contreras, M., Zapatero Osorio, M. R., et al. 2012c, A&A, 542, A105
Minniti, D., Lucas, P. W., Emerson, J. P., et al. 2010, New Astron., 15, 433
Morgan, W. W., Keenan, P. C., & Kellman, E. 1943, An atlas of stellar spectra, with an outline of spectral classification (Chicago: The University of Chicago Press)
Morgan, D. P., West, A. A., Garcés, A., et al. 2012, AJ, 144, 93
Mould, J. R. 1976, A&A, 48, 443
Muraki, Y., Sumi, T., Abe, F., et al. 1999, Prog. Theor. Phys. Suppl., 133, 233
Perryman, M. A. C., de Boer, K. S., Gilmore, G., et al. 2001, A&A, 369, 339
Rayner, J. T., Cushing, M. C., & Vacca, W. D. 2009, ApJS, 185, 289
Rich, R. M., Reitzel, D. B., Howard, C. D., & Zhao, H. 2007, ApJ, 658, L29
Roeser, S., Demleitner, M., & Schilbach, E. 2010, AJ, 139, 2440
Rojas-Ayala, B., Covey, K. R., Muirhead, P. S., & Lloyd, J. P. 2012, ApJ, 748, 93
Saito, R. K., Minniti, D., Dékány, I., et al. 2011, Rev. Mex. Astron. Astrofis., 40, 221
Saito, R. K., Hempel, M., Minniti, D., et al. 2012a, A&A, 537, A107
Saito, R. K., Minniti, D., Dias, B., et al. 2012b, A&A, 544, A147
Sharma, S., Johnston, K. V., Majewski, S. R., et al. 2010, ApJ, 722, 750
Skrutskie, M. F., Cutri, R. M., Stiening, R., et al. 2006, AJ, 131, 1163
Taylor, M. B. 2005, in Astronomical Data Analysis Software and Systems XIV, eds. P. Shopbell, M. Britton, & R. Ebert, ASP Conf. Ser., 347, 29
Tuomi, M., Jones, H. R. A., Barnes, J. R., Anglada-Escudé, G., & Jenkins, J. S. 2014, MNRAS, 441, 1545
Udalski, A., Szymanski, M., Kaluzny, J., Kubiak, M., & Mateo, M. 1992, Acta Astron., 42, 253
West, A. A., Hawley, S. L., Walkowicz, L. M., et al. 2004, AJ, 128, 426
West, A. A., Morgan, D. P., Bochanski, J. J., et al. 2011, AJ, 141, 97
York, D. G., Adelman, J., Anderson, Jr., J. E., et al. 2000, AJ, 120, 1579

Appendix A: Giant and dwarf sequences for VISTA Colours

We estimated VISTA colours of the FGKM dwarf and giant sequences by computing VISTA $ZYJHK_s$ magnitudes for 52 FGKM dwarf and 54 FGKM giant stars from the Infrared Telescope Facility (IRTF) Spectral Library[3]. The IRTF Spectral Library has a collection of $R \sim 2000{-}2500$ FGKM stellar spectra observed with the SpeX spectrograph, with a spectral range of 0.8 to at least 2.5 μm (Cushing et al. 2005; Rayner et al. 2009). The stars in the library were absolutely flux calibrated using 2MASS photometry, with their spectral continuum shape preserved.

The VISTA synthetic magnitude in each filter was estimated using the following equation:

$$m_\lambda = -2.5 \log_{10}\left(\int F_\lambda S_\lambda \, \mathrm{d}\lambda\right) + 2.5 \log_{10}\left(\int F_\lambda^0 S_\lambda \, \mathrm{d}\lambda\right). \quad \text{(A.1)}$$

The second term of the Eq. (A.1) corresponds to the zero point of the magnitude scale. For calculation of the VISTA synthetic magnitudes presented here, the F_λ^0 flux corresponds to that of the Vega spectrum in the CALSPEC library[4] (Bohlin 2014). The response function of the VISTA filter set, S_λ, was calculated from the quantum efficiency curve of the detector and transmission curves for each filter[5]. The VISTA synthetic colours calculated for dwarf and giant stars in the IRTF library are given in Tables A.1 and A.2, respectively.

Using the stars in Tables A.1 and A.2, we fitted the colours of the giant and dwarf sequences using a fifth-order polynomial in $H - K_s$ with the form:

$$\text{colour}\, X = \sum_{i=0}^{5} A_i \, (H - K_s)^i \, . \quad \text{(A.2)}$$

We tabulated the fitted colours of the giant and dwarf sequences as a function of $H - K_s$ colour in Table A.3. The positions of the stellar sequences are shown as orange lines in Fig. 2.

[3] http://irtfweb.ifa.hawaii.edu/~spex/IRTF_Spectral_Library/

[4] http://www.stsci.edu/hst/observatory/crds/calspec.html

[5] http://www.eso.org/sci/facilities/paranal/instruments/vircam/inst.html

Table A.1. VISTA synthetic magnitudes for dwarfs in the IRTF library

Name	Sp. T.	Z	Y	J	H	K_s
HD 108519	F0	7.265	7.231	7.113	6.973	6.935
HD 213135	F1	5.462	5.427	5.263	5.092	5.076
HD 113139	F2	4.444	4.372	4.176	3.998	3.976
HD 26015	F3	5.355	5.305	5.156	5.043	5.057
HD 16232	F4	6.298	6.262	6.081	5.876	5.848
HD 87822	F4	5.611	5.559	5.372	5.194	5.164
HD 27524	F5	6.166	6.144	5.966	5.788	5.767
HD 218804	F5	5.266	5.197	4.983	4.745	4.694
HD 215648	F6	3.577	3.519	3.299	3.075	3.042
HD 126660	F7	3.389	3.349	3.148	2.936	2.883
HD 27383	F8	6.075	5.999	5.799	5.589	5.573
HD 219623	F8	4.963	4.873	4.642	4.386	4.342
HD 176051	F9	4.376	4.303	4.039	3.718	3.667
HD 114710	F9.5	3.427	3.382	3.181	2.988	2.996
HD 109358	G0	3.504	3.438	3.195	2.905	2.876
HD 10307	G1	4.284	4.205	3.964	3.685	3.657
HD 20619	G1.5	6.274	6.168	5.878	5.537	5.475
HD 76151	G2	5.203	5.115	4.855	4.555	4.481
HD 10697	G3	5.442	5.315	5.024	4.695	4.616
HD 214850	G4	4.835	4.747	4.464	4.069	3.972
HD 165185	G5	5.097	5.055	4.831	4.575	4.525
HD 115617	G6.5	3.591	3.522	3.281	2.998	2.985
HD 75732	G8	4.938	4.807	4.504	4.139	4.047
HD 101501	G8	4.397	4.276	3.995	3.665	3.612
HD 145675	K0	5.562	5.438	5.135	4.796	4.743
HD 10476	K1	4.269	4.139	3.809	3.405	3.318
HD 3765	K2	6.173	6.025	5.678	5.262	5.183
HD 219134	K3	4.586	4.358	3.955	3.444	3.333
HD 45977	K4	7.578	7.403	7.033	6.555	6.455
HD 36003	K5	6.199	5.996	5.588	5.031	4.915
HD 201092	K7	4.014	3.824	3.427	2.875	2.736
HD 237903	K7	6.813	6.562	6.108	5.499	5.376
HD 19305	M0	7.199	6.932	6.471	5.837	5.671
HD 209290	M0.5	6.992	6.676	6.174	5.544	5.348
HD 42581	M1	5.866	5.555	5.073	4.465	4.277
HD 36395	M1.5	5.746	5.407	4.893	4.215	4.032
Gl 806	M2	8.107	7.786	7.304	6.741	6.581
HD 95735	M2	4.928	4.611	4.125	3.611	3.435
Gl 381	M2.5	7.895	7.522	6.993	6.438	6.236
Gl 581	M2.5	7.545	7.163	6.649	6.123	5.887
Gl 273	M3.5	6.679	6.225	5.668	5.149	4.915
Gl 388	M3	6.334	5.936	5.403	4.841	4.645
Gl 213	M4	8.141	7.665	7.112	6.641	6.415
Gl 299	M4	9.392	8.933	8.377	7.958	7.711
Gl 51	M5	9.799	9.225	8.575	8.029	7.758
Gl 406	M6	8.613	7.819	7.054	6.483	6.131
GJ 1111	M6.5	9.761	8.954	8.181	7.648	7.295
Gl 644C	M7	11.357	10.533	9.741	9.224	8.862
LP 412-31	M8	13.672	12.681	11.732	11.089	10.675
DENIS-P J1048-3956	M9	11.456	10.389	9.459	8.933	8.537
LP 944-20	M9	12.933	11.718	10.664	10.052	9.605
BRIB 0021-0214	M9.5	14.195	12.995	11.843	11.132	10.625

Table A.2. VISTA synthetic magnitudes for giants in the IRTF library

Name	Sp. T.	Z	Y	J	H	K_s
HD 89025	F0	2.956	2.914	2.763	2.606	2.578
HD 21770	F4	4.683	4.645	4.473	4.295	4.275
HD 17918	F5	5.671	5.599	5.412	5.224	5.215
HD 124850	F7	3.431	3.352	3.121	2.883	2.862
HD 220657	F8	3.913	3.809	3.521	3.196	3.093
HD 6903	F9	4.925	4.813	4.535	4.216	4.155
HD 21018	G1	5.305	5.146	4.827	4.475	4.391
HD 88639	G3	4.988	4.837	4.504	4.111	4.049
HD 108477	G4	5.299	5.135	4.799	4.402	4.312
HD 193896	G5	5.305	5.095	4.712	4.265	4.151
HD 27277	G6	6.808	6.587	6.215	5.795	5.715
HD 182694	G7	4.865	4.729	4.395	3.988	3.888
HD 16139	G7.5	6.755	6.549	6.173	5.715	5.595
HD 135722	G8	2.174	2.006	1.645	1.153	1.034
HD 104979	G8	3.108	2.944	2.589	2.105	2.013
HD 122563	G8	4.969	4.785	4.392	3.862	3.765
HD 222093	G9	4.692	4.508	4.123	3.619	3.517
HD 100006	K0	4.511	4.295	3.893	3.363	3.261
HD 9852	K0.5	6.183	5.859	5.356	4.755	4.605
HD 25975	K1	4.979	4.849	4.522	4.098	4.028
HD 91810	K1	5.497	5.256	4.831	4.303	4.169
HD 36134	K1	4.415	4.209	3.797	3.259	3.165
HD 124897	K1.5	–1.535	–1.759	–2.203	–2.853	–2.987
HD 137759	K2	1.998	1.756	1.314	0.747	0.611
HD 132935	K2	5.206	4.931	4.441	3.779	3.614
HD 2901	K2	5.653	5.391	4.931	4.325	4.225
HD 99998	K3	3.037	2.717	2.159	1.414	1.215
HD 35620	K3	3.637	3.336	2.845	2.227	2.048
HD 178208	K3	5.185	4.892	4.411	3.821	3.674
HD 221246	K3	4.675	4.364	3.863	3.203	3.055
HD 114960	K3.5	4.852	4.558	4.088	3.471	3.316
HD 207991	K4	4.909	4.548	3.983	3.209	3.005
HD 181596	K5	5.721	5.357	4.799	4.073	3.867
HD 120477	K5.5	2.172	1.823	1.268	0.532	0.316
HD 3346	K6	3.126	2.786	2.225	1.452	1.213
HD 194193	K7	4.025	3.646	3.064	2.252	2.022
HD 213893	M0	4.812	4.444	3.885	3.125	2.916
HD 204724	M1	2.488	2.116	1.593	0.875	0.618
HD 120052	M2	2.894	2.488	1.864	1.022	0.747
HD 219734	M2.5	2.519	2.098	1.493	0.681	0.428
HD 39045	M3	3.621	3.181	2.551	1.719	1.446
HD 28487	M3.5	3.851	3.324	2.659	1.781	1.485
HD 27598	M4	4.038	3.562	2.953	2.128	1.856
HD 214665	M4	2.556	1.886	1.114	0.156	–0.182
HD 4408	M4	2.539	2.043	1.405	0.546	0.239
HD 204585	M4.5	2.294	1.691	1.062	0.278	0.026
HD 175865	M5	0.496	–0.128	–0.769	–1.570	–1.811
HD 94705	M5.5	1.822	1.089	0.401	–0.429	–0.763
HD 18191	M6	1.739	0.966	0.252	–0.622	–0.938
HD 196610	M6	1.653	0.816	0.144	–0.649	–0.945
HD 108849	M7	2.488	1.362	0.495	–0.332	–0.722
HD 207076	M7	1.186	0.195	–0.500	–1.206	–1.477
IRAS 21284-0747	M8	8.752	7.262	6.107	5.373	4.819
BRIB 1219-1336	M9	10.689	9.446	8.556	7.919	7.447

Table A.3. VISTA colours as a function of $(H - K_s)$ for dwarfs and giants.

Dwarfs			Giants			
$(Z-Y)$	$(Y-J)$	$(J-H)$	$(Z-Y)$	$(Y-J)$	$(J-H)$	$(H-K_s)$
0.065	0.181	0.169				–0.015
0.052	0.176	0.162				–0.005
0.046	0.178	0.168	0.027	0.146	0.126	0.005
0.046	0.186	0.183	0.051	0.177	0.176	0.015
0.051	0.198	0.205	0.072	0.207	0.221	0.025
0.059	0.214	0.234	0.091	0.234	0.263	0.035
0.070	0.232	0.266	0.109	0.260	0.301	0.045
0.084	0.253	0.300	0.125	0.284	0.337	0.055
0.100	0.274	0.335	0.140	0.307	0.370	0.065
0.117	0.296	0.370	0.154	0.328	0.401	0.075
0.136	0.318	0.405	0.168	0.348	0.431	0.085
0.155	0.340	0.437	0.182	0.368	0.460	0.095
0.174	0.362	0.467	0.195	0.386	0.487	0.105
0.194	0.383	0.494	0.209	0.404	0.514	0.115
0.214	0.403	0.517	0.223	0.421	0.540	0.125
0.233	0.422	0.537	0.238	0.438	0.565	0.135
0.253	0.439	0.553	0.253	0.454	0.589	0.145
0.273	0.456	0.565	0.269	0.470	0.613	0.155
0.293	0.472	0.573	0.286	0.486	0.637	0.165
0.313	0.486	0.578	0.304	0.501	0.659	0.175
0.333	0.500	0.580	0.324	0.516	0.681	0.185
0.354	0.513	0.578	0.344	0.531	0.703	0.195
0.374	0.525	0.574	0.366	0.545	0.723	0.205
0.396	0.537	0.567	0.389	0.559	0.742	0.215
0.418	0.549	0.559	0.414	0.574	0.761	0.225
0.441	0.560	0.549	0.439	0.588	0.778	0.235
0.465	0.572	0.539	0.467	0.602	0.794	0.245
0.490	0.585	0.528	0.495	0.615	0.808	0.255
0.516	0.598	0.517	0.525	0.629	0.820	0.265
0.544	0.612	0.507	0.556	0.643	0.831	0.275
0.574	0.628	0.498	0.589	0.656	0.840	0.285
0.605	0.644	0.491	0.623	0.670	0.847	0.295
0.637	0.662	0.485	0.658	0.683	0.852	0.305
0.672	0.682	0.482	0.693	0.697	0.854	0.315
0.707	0.703	0.482	0.730	0.710	0.855	0.325
0.745	0.726	0.484	0.768	0.723	0.853	0.335
0.783	0.751	0.490	0.807	0.737	0.849	0.345
0.823	0.778	0.498	0.846	0.750	0.843	0.355
0.864	0.806	0.510	0.885	0.763	0.834	0.365
0.906	0.836	0.525	0.925	0.777	0.824	0.375
0.947	0.867	0.543	0.965	0.791	0.811	0.385
0.989	0.899	0.563	1.005	0.805	0.798	0.395
1.030	0.932	0.585	1.045	0.819	0.782	0.405
1.069	0.964	0.609	1.085	0.834	0.766	0.415
1.106	0.997	0.633	1.124	0.849	0.748	0.425
1.141	1.028	0.657	1.162	0.865	0.731	0.435
1.171	1.058	0.679	1.199	0.881	0.713	0.445
1.197	1.086	0.699	1.236	0.898	0.696	0.455
1.217	1.110	0.714	1.270	0.916	0.680	0.465
1.230	1.129	0.724	1.304	0.935	0.666	0.475
1.234	1.144	0.726	1.335	0.956	0.655	0.485
1.229	1.151	0.718	1.364	0.978	0.647	0.495
1.212	1.150	0.698	1.391	1.001	0.644	0.505
1.182	1.140	0.663	1.416	1.026	0.646	0.515
			1.437	1.054	0.654	0.525
			1.456	1.084	0.670	0.535
			1.471	1.116	0.695	0.545
			1.482	1.151	0.731	0.555